Components of the Creep Strength of Welds

M. Murugananth and H.K.D.H. Bhadeshia
Department of Material Science and Metallurgy,
University of Cambridge, Pembroke street,
United Kingdom CB2 3QZ
contact mail id: mm322@cus.cam.ac.uk
Ph: +44-(01223) 334495

Abstract

Modern power plant steels and welding alloys, designed to resist creep deformation at high temperatures, contain a myriad of alloying elements and a microstructure which has six or more phases. It has not therefore been possible to identify the precise role of each chemical and microstructural component in determining the ultimate creep properties.

In this work, we have used a combination of models and a knowledge of the mechanical properties and microstructure, to factorise the long–term creep rupture strength into individual contributions, for example due to solution strengthening, precipitate strengthening *etc.* The factorisation is non–linear and relies on thermodynamic and mechanical property models. The work is general in the sense that it covers all c ommon ferritic steels and welding alloys of the type used in the construction of power plant.

An assessment is included of some of the most modern alloys with interesting conclusions on the factors making major contributions to the long–term creep rupture strength.

Introduction

Ferritic steels are used extensively in the construction of power plant for electricity generation [1–7]. Intrinsic properties like low thermal expansion coefficient and a high thermal conductivity of ferrite makes them suitable for high–temperature applications. Nickel alloys do have a sufficiently low expansion coefficient, but are expensive.

The main design requirement is that the ferritic steel should resist creep and oxidation, but should at the same time be easy to fabricate into very large components. This in turn means that they should be weldable and that any welds must be sufficiently robust to meet the creep requirements. There are in this context, major international research programmes with the aim of designing novel steels and welding alloys [1–7]. The design procedure is based on scientific and engineering experience and the use of a variety of models, for example, phase stability calculations, the assessment of diffusion coefficients, kinetic theory associated with precipitation reactions, elementary creep theory and complex neural network models to express the creep strength as a function of a very large number of variables.

Elementary creep theory, such as that used in the construction of Ashby diagrams, is useful in gaining insight into the creep mechanisms, but is unable to predict the creep behavior of multicomponent steels as a function of the chemical composition, heat treatment and service conditions. Neural network models based on vast experimental datasets are able to cope with such complexity and help visualise the nature of the interactions between variables in a way that is impossible with any other method of pattern recognition. They are, nevertheless, empirical making it difficult to extract physical mechanisms.

The creep resistance of ferritic steels, over long periods of time at elevated temperatures, relies on the presence of stable precipitates which interfere with the climb and glide of dislocations, and which retard the coarsening rate of the microstructure as a whole, for example, the size and shape of martensite or bainite plates. The nature of the precipitate clearly depends on the detailed composition and heat treatment, but the variety is impressive, including Fe_3C (cementite), $M_{23}C_6$, M_7C_3, M_6C, M_2X, M_3C, Laves, M_5C_2 and Z-phase. There may typically be five or more of these precipitate phases in a creep–resistant steel.

Precipitation also affects the solute left in solution in the ferrite; solution strengthening is believed to be an important component of the long–term creep life. It would be incredibly useful to know quantitatively, the contribution

made by each of the precipitate phases, and by solution strengthening due to each solute, to the long–term creep strength. There are currently no models capable either of extracting this information from experimental data or of making quantitative predictions. The purpose of the present work was to attempt precisely this task, using a neural network model but with inputs chosen to represent precipitates and solutes.

The work described here is based on steel plates rather than weld deposits. It has been demonstrated in previous work that as far as the creep–rupture life is concerned, there is no essential difference between weld metal and wrought metal [8].

Inputs to the model

Artificial neural network models used in this work were constructed based on rupture time and temperature, composition, heat treatment, precipitate fraction and wt% dissolved solutes. Detailed description about the database and construction of the neural network model can be found elsewhere [8, 9]. The models were previously used to factorise the strength of $2\frac{1}{4}$Cr1Mo steel and NF616 [9].

The same models in combination with thermodynamics were used here for factorisation of creep–rupture strength of HCM12A at 600 °C after 10^5 h.

HCM12A

HCM12A is a high–chromium creep–resistant martensitic steel intended for use in the temperature range of 600 °C as a power plant material. Its chemical composition is given in table 1. This is categorised under tungsten alloyed heat–resisting steels with a notably low molybdenum content than its predecessor HCM12 [2]. Alloying with tungsten could result in formation of Laves phases which hinder the coarsening of $M_{23}C_6$ [10, 11].

Published calculations of the phase diagram of HCM12A [12] indicate the presence of M_2X (identified in CALPHAD notation as HCP_A3) as an equilibrium phase at the temperature of interest. We have investigated this and found that the prediction of M_2X is an artifact since FCC (face–centered cubic) or copper as a phase is excluded when conducting calculations below Ae_1 temperature. This is acceptable for most steels, but not for HCM12A that contains copper, which precipitates as an FCC phase. Excluding FCC in the the computation results incorrectly in HCP_A3 copper.

The analysis here is presented for an alloy normalised at 1070 °C for 1 h and tempered at 770 °C for 1 h. In both cases the cooling to room temperature is assumed to be in air. After 10^5 h it is expected to have a creep strength of 120–140 MPa at 600 °C [2]. Our calculations using artificial neural network predicted a 10^5 h rupture strength of 123±10 MPa at 600 °C .

Calculations show that vanadium in someway influences the strengthening contribution of tungsten. At zero concentration of vanadium, the contribution to strength by tungsten reduces (fig. 1). This influence need not be just due to the presence of vanadium in solid solution or its carbide. Studies have shown that the presence of carbide forming elements like vanadium can interact with interstitial elements like carbon and nitrogen to cause exaggerated solid solution strengthening [13]. The absence of vanadium neither affects Laves phase fractions, wt% of dissolved tungsten or dissolved molybdenum, but only eliminates vanadium nitride and dissolved vanadium (table 2) and the exaggerated solid solution strengthening. However, M_2X rich in chromium and nitrogen appears on removal of vanadium (table 2). But, calculations show that amount of M_2X is constant at 99.6 moles even with variation of tungsten concentration, thus having no effect on tungsten's strength contribution. Hence it would be appropriate to calculate the strength contribution due to tungsten in the absence of vanadium, which clearly removes the synergic strengthening effect due to vanadium that is added implicitly to that of tungsten. Thus, tungsten contributes 7.96 MPa in total at zero concentration of vanadium. Since dissolved tungsten is the only component varying in the shaded region of fig. 2, 4.3 MPa of the 7.96 MPa can be attributed to solution strengthening from tungsten. Hence, the remaining 3.66 MPa comes from Laves phases and dissolved molybdenum.

Similarly, vanadium and tungsten influence the strength contribution of niobium and molybdenum (fig. 1). Thus, the contribution to strength due to niobium should be:

$$\sigma_{Nb} = \sigma_{Nb|V,W} - \sigma_{Nb|V=0,W} - \sigma_{Nb|V,W=0} = 14.68 - 6.17 - 6 = 2.51 \text{ MPa} \quad (1)$$

where $\sigma_{Nb|V,W}$, $\sigma_{Nb|V=0,W}$ and $\sigma_{Nb|V,W=0}$ are the strength contributions due to niobium at 0.2V-1.92W wt%, 0V-1.92W wt% and 0.2V-0W wt% respectively. Calculations for molybdenum after removing the effect of vanadium and tungsten give 2.29 MPa.

The presence of dissolved vanadium and

its nitride contributes 78.8 MPa to the total strength. It should be noted that the total strength of HCM12A is a synergic effect of both tungsten and vanadium, whereas the individual contributions of W, Nb and Mo are always small. The individual contributions of dissolved vanadium or vanadium nitride could not be separated because other factors did not remain constant.

It has long been known that chromium hardly contributes to any strengthening at 600 °C (fig. 4). Chromium is added to the steel mainly for corrosion resistance and hardenability [14].

Having calculated the contributions due to all the alloying elements, the remaining contribution to strength of HCM12A comes from Fe and microstructure (123-91.56=31.55 MPa).

The pie chart in fig. 5 summarises the strength contributions from individual components in the alloy.

Conclusions

The creep–rupture strength of a material is not a simple linear function of composition, temperature and time. Hence, this non–linearity which is captured by the neural networks was used in combination with thermodynamics to find the strength contribution from components of the alloy.

High chromium heat–resisting steel like HCM12A have vanadium as one of the main alloying elements that contributes to more than half of its high temperature strength. Chromium is added in large concentrations since a minimum of 11 wt% is required for resisting corrosion and high temperature oxidation. Copper is added for improving the toughness of the alloy.

Finally, this alloy relies heavily on vanadium and its nitride for its long term strength at 600 °C. All the other precipitates must play a significant role during the early stages of creep life but we are not able to address this, since our calculations rely on equilibrium.

Acknowledgements

The authors wish to acknowledge the Nehru Trust for Cambridge University and Cambridge Commonwealth Trust for the funding towards this project. They are also greatful to Professors H. Cerjak (Graz Technical University, Austria) and H. O. Andrén (Chalmers University, Sweden) for their useful comments.

C	Si	Mn	P	S	Cr
0.12	0.04	0.63	0.013	0.001	10.75
Mo	W	Ni	Cu	V	Nb
0.39	1.92	0.28	0.9	0.21	0.04
N	B				
0.062	0.001				

Table 1: Composition of HCM12A

	0.2 wt% V	0 wt% V
Mole fraction of precipitates		
$M_{23}C_6$	3.14×10^{-2}	3.147×10^{-2}
Laves	1.087×10^{-2}	1.023×10^{-2}
NbN	4.80×10^{-4}	4.81×10^{-4}
M_2X	5.64×10^{-3}	0
VN	4.46×10^{-3}	0
Dissolved Solutes / wt%		
W_{ss}	0.596	0.653
V_{ss}	0.0064	0

Table 2: Phase fractions in absence and presence of vanadium in HCM12A base composition. W_{ss} and V_{ss} denote dissolved tungsten and vanadium concentrations respectively.

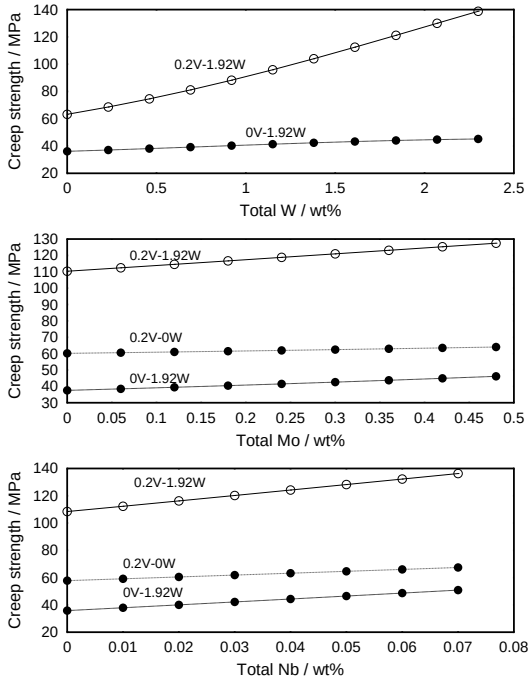

Figure 1: Influence of vanadium and tungsten on strength contribution of other alloying elements in HCM12A

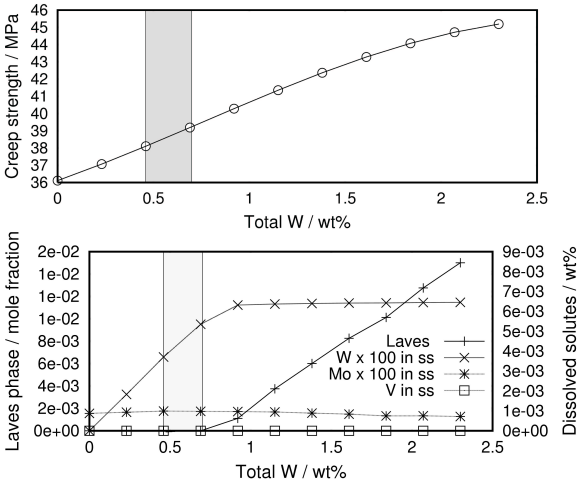

Figure 2: Effect of tungsten and its precipitates on creep strength at zero vanadium concentration.

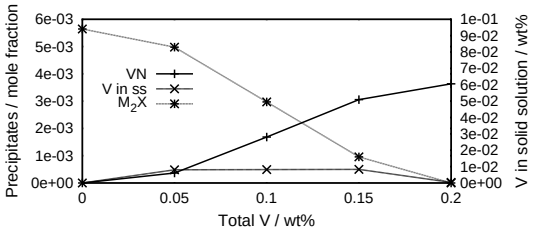

Figure 3: Phase fractions of VN and M_2X and wt% of dissolved vanadium.

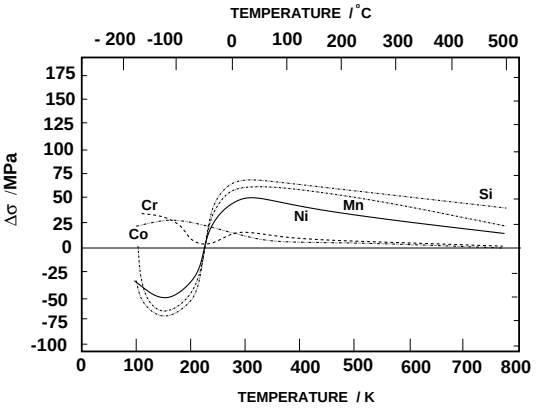

Figure 4: Sold–solution hardening and softening in iron–base alloys, adapted from Leslie [15].

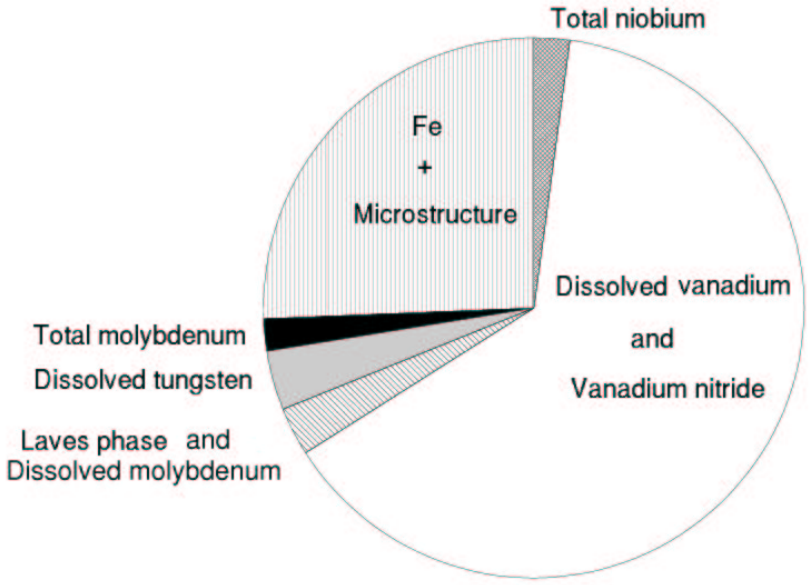

Figure 5: Pie-chart showing strength contribution from various components of HCM12A. The total strength of HCM12A is 123 MPa at 600 °C after 10^5 h.

References

[1] F. Abe, M. Igarashi, N. Fujitsuna, K. Kimura, and S. Muneki. In Lecomte-Beckers *et al.*, editor, *6th Leige Conference on Materials for Advance Power Engineering*, pages 259–268, October 1998.

[2] H. Cerjak, H. Peter, and B. Schaffernak. *ISIJ International*, 39(9):874–888, 1999.

[3] H. K. D. H. Bhadeshia. *ISIJ International*, 41(6):626–640, 2001.

[4] F. Masuyama. *ISIJ International*, 41(6):612–625, 2001.

[5] K. Maruyama, K. Sawada, and J. Koike. *ISIJ International*, 41(6):641–653, 2001.

[6] T. Fujita. In E. Metcalfe, editor, *New steels for Advanced plant up to 620 °C* , pages 190–200, 58, Abingdon Road, Drayton, Oxon, OX14 4HP, UK, May 1995. National Power, PicA.

[7] T. Fujita. *Metal Progress*, 130:33–36, 1986.

[8] D. Cole, C. Martin-Moran, A. G. Sheard, H. K. D. H. Bhadeshia, and D. J. C. MacKay. *Science and Technology of Welding and Joining*, 5:81–90, 2000.

[9] M. Murugananth. and H. K. D. H. Bhadeshia. In *Mathematical Modelling of Weld Phenomena*, VI, IOM Communications Ltd, 1 Carlton House Terrace, London SW1Y 5DB. Institute of Materials. To be published.

[10] C. A. Parsons. The steam turbine. In *Rede Lecture*, Cambridge, U.K, 1911. Cambridge University Press.

[11] F Abe. In T Sakai. and H. G. Suzuki., editors, *Fourth International Conference on Recrystallisation and Related Phenomena*, pages 289–294. The Japan Institute of Metals, 1999.

[12] J Hald. In E. Metcalfe, editor, *New steels for Advanced plant upto 620 °C* , pages 152–173, 58, Abingdon Road, Drayton, Oxon, OX14 4HP, UK, May 1995. National Power, PicA.

[13] J. D. Baird. and A Janieson. *Journal of Iron Steel Inst.*, 210:841, 1972.

[14] Y. Sawaragi, A. Iseda, K. Ogawa, F. Masuyama, and T. Yokoyama. In E. Metcalfe, editor, *New steels for Advanced plant upto 620 °C* , pages 45–55, 58, Abingdon Road, Drayton, Oxon, OX14 4HP, UK, May 1995. National Power, PicA.

[15] W. C. Leslie. *The Physical Metallurgy of Steels.* McGraw-Hill, London, 1981.